A Ultra-lightweight ILS Receiving Payload Base on Multi-rotor UAV for Flight Inspection

Wang Pengfei
System Engineer
Aviation Data Communication Corporation
Beijing, China
Tel: +86 13426013890
E-mail: wangpf@adcc.com.cn

Rong Yi
Hardware Engineer
Beijing Sky Aviation
Beijing, China
Tel: +86 13901072051
E-mail: yi.rong@bsac.com.cn

Li Xiaoqiang
Software Engineer
Beijing Sky Aviation
Beijing, China
Tel: +86 13488685423
E-mail: xiaoqiang.li@bsac.com.cn

Ji Yue
Software Engineer
Aviation Data Communication Corporation
Beijing, China
Tel: +86 13810526605
E-mail: jiy@adcc.com.cn

ABSTRACT

A lot of Unmanned Aerial Vehicle (UAV) systems have been developed as measurement equipment for NAVAID test applications in recent years. For instance, drones equipped with cameras are used for light verification and drones equipped with ILS receivers are used for ILS facility inspection.

Compared with crewed aircraft systems, UAV systems have the advantages of convenient maintenance, easy operation and low cost. However, due to the size and load capacity of the UAV, R&D Engineers need to develop a special highly integrated lightweight receiver payload and adapt to the specific electromagnetic environment of the UAV, for example propeller modulation.

The institution represented by author has developed variety of UAV system for NAVAID test in a decade, include fixed-wing unmanned aircraft, composite wing UAV and multi-rotor UAV. Recently an ultra-lightweight and highly integrated ILS receiving payload was developed and tested in flight at several airports in China.

This article presents the research and design of this ILS test system RFIS and illustrates the flight test result. A ultra-lightweight ILS receiving payload base on multi-rotor UAV is introduced and UAV application test is discussed.

INTRODUCTION

The drone-based flight inspection system has become a future development trend for airport facility testing. In recent years, countries around the world have been actively developing their own drone flight inspection systems, with diverse drone

platforms being used. These platforms include fixed-wing drones, composite wing drones, and multi-rotor drones, among others. For example, a company has used a fixed-wing drone combined with a commercial ILS analyzer to construct a medium-sized flight inspection system. Meanwhile, multiple countries are also trying to use multi-rotor drone platforms to build simple flight test systems for ILS, VOR, and other tests.

Although fixed-wing drones have longer flight times and greater flying distances, due to their larger size, take-off and landing require runway support, and they use fossil fuels as their power source, their application is still limited.

On the other hand, although the flight time of multi-rotor drones is relatively short and the flying distance is also relatively close, they generally use battery power and have the advantages of simple operation and low requirements for take-off and landing sites. This makes them more convenient for executing simple critical flight tests for ILS/VOR facility.

Ten years ago, the author's institution attempted to develop a flight inspection system based on a medium-sized fixed-wing UAV with the aim of replacing crewed aircraft for flight inspection. In this system, we used the same payload as crewed aircraft. Subsequently, we adopted modular payload and installed it on small composite-wing UAV, successfully conducting practical flight inspection.

Recently, we have collaborated with the Civil Aviation Department of Hong Kong to jointly develop a flight inspection system based on multi-rotor drone, and conducted flight testing at the Hong Kong International Airport successfully.

Due to the limited payload capacity of the multi-rotor drone, we have developed a ultra-lightweight ILS/VOR receiver that is deeply integrated with the existing RTK subsystem and data link subsystem of the drone, forming a lightweight payload that meets the testing requirements for ILS/VOR. This article focuses on the development process of the ILS/VOR payload and demonstrates the actual flight test results of the ILS/VOR facility.

DEVELOPMENT OF PAYLOAD SYSTEM

Payload Overview

Figure 1. RFIS Overview

The ILS/VOR flight inspection system (RFIS) is developed based on the integration of the DJI MATRICE 350 RTK drone. The maximum payload capacity of the drone is 2.5kg, and its nominal maximum flight time is 55 minutes. The drone integrates a GNSS RTK subsystem, and in the RTK Fix mode, the horizontal positioning accuracy is 1cm + 1ppm, and the vertical positioning accuracy is 1.5cm + 1ppm. The RFIS block diagram consists of the following main components:

- GNSS Antenna;
- UM982 GNSS Receiver Unit;
- Data Link Unit;
- FCM Flight Control Module;
- PSDK Adapter;
- ILS/VOR Receiver;
- ILS Antenna;

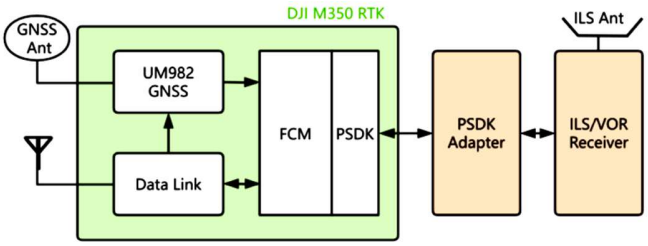

Figure 2. RFIS Block Diagram

Note: The PSDK adapter, ILS/VOR receiver, and ILS antenna are external payloads. The remaining functional units have been integrated within the MATRICE 350 RTK drone.

ILS/VOR Receiver

The block diagram of the ILS/VOR receiver is as follows:

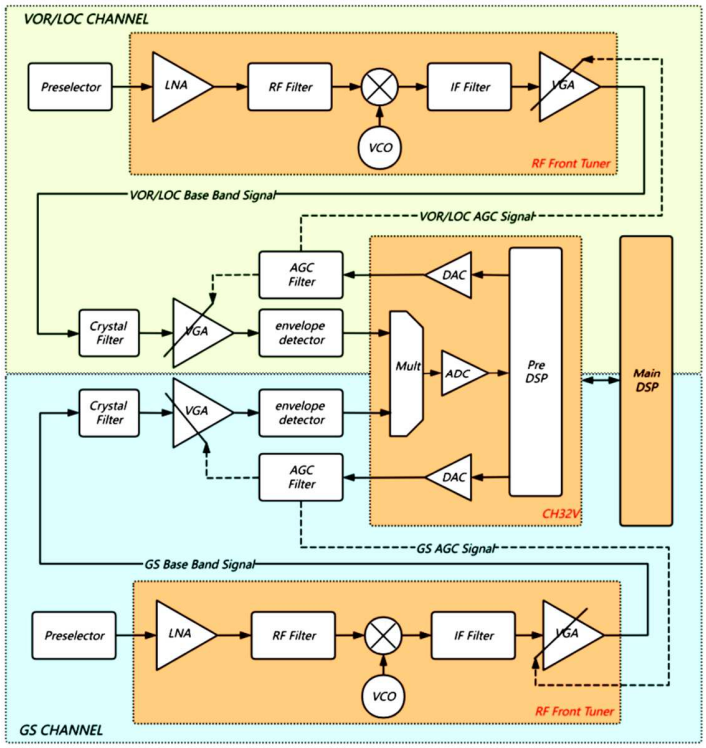

Figure 3. ILS/VOR Receiver Block Diagram

It includes two receiving channels that can receive LOC and GS signals simultaneously. To improve integration, RF front-end tuners are used, which internally integrate low-noise amplifier, RF filter, VCO, mixer, intermediate-frequency filter, and VGA module. A preselector is used to filter out external interference for improving the receiver's anti-jamming capability.

The receiver's main control unit tunes and configures the RF front-end tuners through an IIC bus, mainly parameters including LNA gain, tuning frequency, mixer gain, etc.

The RF front-end chip outputs a 10.7MHz intermediate-frequency signal, which is further filtered by an external crystal filter to remove external interference and is then amplified again by a VGA. The intermediate-frequency signal output by the VGA undergoes AM demodulation through a envelope detector, resulting in LOC base band signal (BB Signal) or GS base band signal.

The design goal of ILS/VOR receiver is to improve integration, enhance dynamic signal measurement capability, and achieve dual-channels reception capability. Regarding dynamic signal measurement capability, this design utilizes an analog automatic gain control (AGC) loop, which can measure the strength of RF signals in real time and generate a continuous analog gain control voltage through a digital-to-analog converter (DAC), thereby improving the stability performance of intermediate frequency signals in dynamic environments.

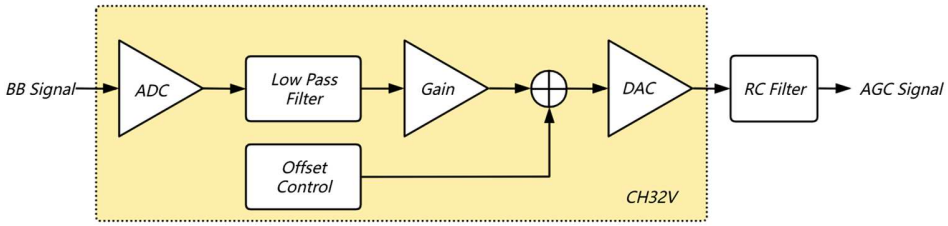

Figure 4. Receiver AGC Function Diagram

There is a significant difference between the AGC loop in this design and traditional software-defined radio (SDR) design philosophy. Software-defined radio (SDR) typically utilizes a step-by-step gain control mode, which performs well in static signal reception environment. However, for the reception of ILS and VOR signals during flight, to obtain high-precision observation values, we must strive to ensure that the signal amplitude in the internal RF channel of the receiver remains stable. The traditional step-by-step gain control mode can cause an amplitude jump during gain switching, which can lead to errors in observation measurements such as ILS DDM.

Digital Signal Processing of ILS

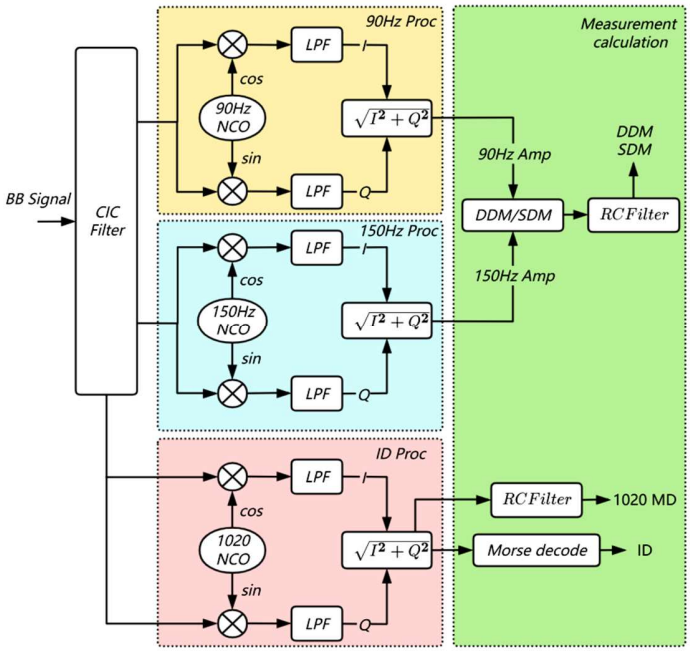

Figure 5. ILS Digital Signal Processing Flow Diagram

The digital signal processing flow for ILS receiving involves a sampling operation to reduce the sampling rate to match the bandwidth of the ILS base band signal, in accordance with the Nyquist sampling theorem. In this step, a CIC comb filter is applied to achieve a reduction in the sampling rate. A suitable sampling rate not only provides the basis for designing efficient IIR (Infinite Impulse Response) filter, but also reduces the computational requirement for digital signal processing.

ILS digital signal processing mainly includes: 90Hz signal amplitude measurement, 150Hz signal amplitude measurement, 1020Hz signal amplitude measurement, and finally the DDM, SDM, ID parameter calculation. For the amplitude

measurement of specific frequency signals, we use IQ down converter combined with IQ envelope detector to achieve it. The accuracy of amplitude measurement is mainly determined by the performance of the low-pass filter(LPF) and the computational accuracy of IQ envelope detector.

In this design, we have chosen a 4th-order IIR filter as the LPF. Additionally, considering that the IQ envelope detector has a large computational burden, we have also optimized the algorithm for this part to improve processing efficiency.

IQ envelope detection：

$$A_{env} = \sqrt{I^2 + Q^2}$$

Algorithm optimization can be achieved through Robertson approximation [1]:

$$A_{env} \approx MAX\left(|I| + \frac{|Q|}{2}, |Q| + \frac{|I|}{2}\right)$$

Digital Signal Processing of VOR

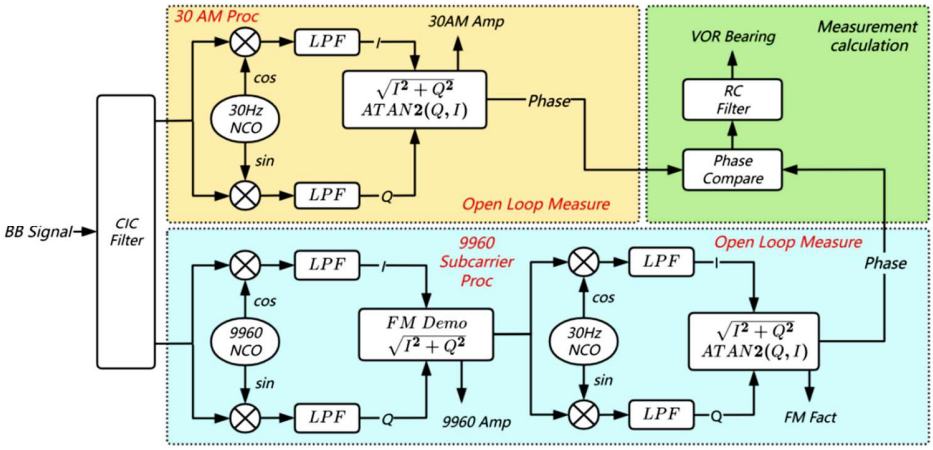

Figure 6. VOR Digital Signal Processing Flow Diagram (Open Loop Measurement)

Most VOR digital signal processing uses open-loop measurement method, which directly employ the ATAN2(Q,I) function for full-phase measurement within $\pm 180^\circ$ region. The advantage of this method lies in its simple and clear structure, however, what many designers may not realize is that the phase discriminator outputs are linear only near the 0^o region in the presence of noise. Using open-loop measurement, the measurement deviation at certain azimuths reaches about 0.1°, especially at azimuths close to 180°.

To address the measurement error caused by phase detector non-linearity, it is necessary to ensure that the phase detector operates as close to 0° as possible. An obvious solution is to adopt a phase lock loop(PLL) measurement method, which is a closed-loop measurement method.

The phase difference output by the phase discriminator is processed by the loop filter and input to the phase shifter. The phase shifter controls the frequency value of the local 30Hz NCO so as to achieve synchronous locking of the 30Hz phase output by the local NCO with the VOR 30Hz signal. By comparing the phase difference between two phase shifters, we can obtain VOR bearing data.

When both PLL loops are locked, their phase discriminators operate in the 0° region, ensuring linear performance of phase discriminators , thereby eliminating measurement errors.

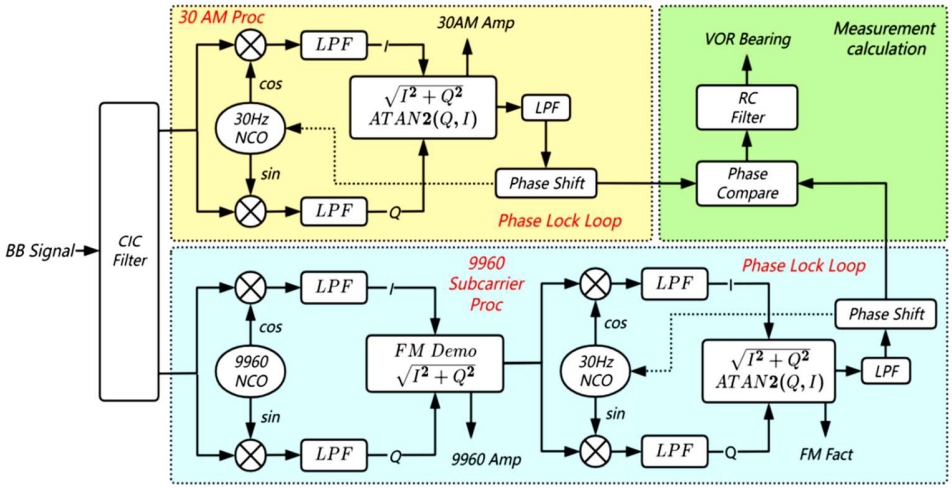

Figure 7. VOR Digital Signal Processing Flow Diagram (Closed-loop Measurement)

ILS/VOR Receiver Assembling

The ILS/VOR receiver is assembled with carbon board. Carbon board is lightweight and has a certain electromagnetic shielding effect, which is more suitable for integration and assembling of drone payload devices. The ILS/VOR Receiver size: 13cm x 10cm x 4cm and **weight : 0.22kg**.

This receiver is tailored for ILS near-field testing tasks and has a dynamic range for receiving signals that is different from that of conventional civil aviation navigation receivers. In practical testing, the received signal strength ranges from -5dBm to -80dBm. In laboratory testing, the receiver's sensitivity is approximately -92dBm. If wanting to achieve higher sensitivity, we may have to compromise some of the strong signal receiving capabilities or add other gain modules. However, it is clear that for this test, we do not require high sensitivity but rather strong signal receiving capability.

Figure 8. ILS/VOR Receiver

ILS/VOR Antenna Design

GS signal frequency is approximately three times LOC signal frequency, it's possible to design an antenna that is compatible with both LOC and GS frequency bands. A specialized dipole antenna with appropriate V-shaped bending was designed and implemented. The purpose of the V-shaped bending is to avoid the original null problem at 0 and 180 degrees of conventional dipole antennas pattern.

For dipole antennas, to improve antenna efficiency, a balun device is needed to perform differential to single-ended matching. A balun device is essentially a transformer.In addition, to reduce the weight of the antenna, the antenna elements are made of aluminum tube material, and LEMO quick connectors are used for easy installation.

Figure 9. ILS/VOR Antenna

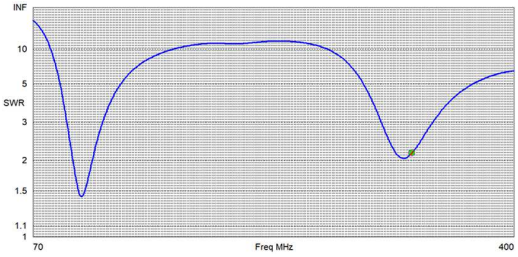

Figure 10. ILS/VOR Antenna SWR

PSDK Adapter Design

In order to support developers in developing payload devices that can be mounted on DJI drones, DJI provides a development kit Payload SDK (PSDK) and development accessories X-Port, SkyPortV2 and SDK Round Ribbon Cable, etc. It is convenient for developers to develop payload that can be mounted on DJI drones by using the resources such as power supply, communication link and status information on DJI drones. [2]

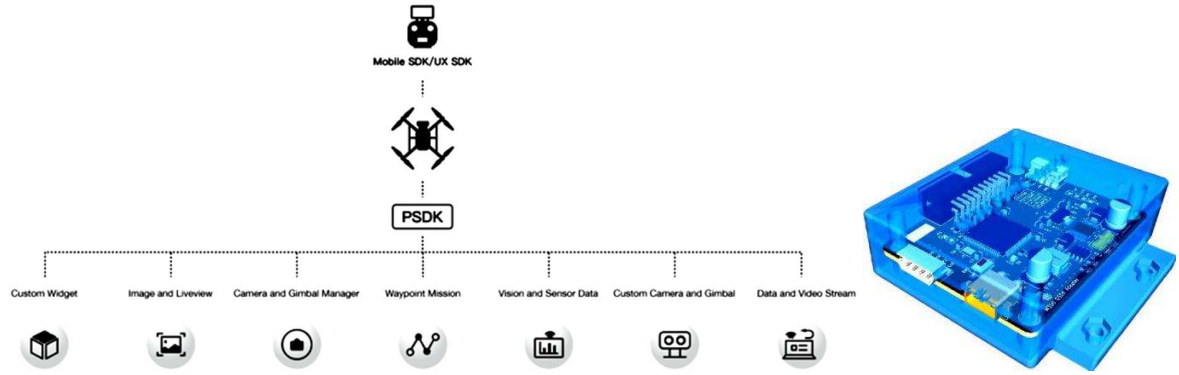

Figure 11. PSDK Structure and PSDK Adapter

Using PSDK to develop payload can fully leverage the positioning capabilities of DJI drones and needn't additional onboard data link. Adding additional data link would not only increase payload weight, but also additional radio emissions could potentially interfere ILS/VOR receiver.

The designed PSDK Adapter has following functions:

- Subscribing GNSS data from the DJI drone;
- Receiving measurement values from the ILS/VOR receiver via a serial port;
- Receiving frequency words sent by the ground MSDK and tuning the ILS/VOR receiver via serial port;
- Synchronizing GNSS data and ILS/VOR data, and sending them to the ground MSDK component via PSDK serial port.

FLIGHT TEST INTRODUCTION

From July 2023 to June 2024, RFIS system has conducted four mission tests at Chengde airport and Hong Kong airport, covering multiple subject tests in each mission test.

The flight testing include：

- LOC ZONE 4 and ZONE 5 roll out subject;
- LOC width and symmetric subject;

- GS clearance subject;
- ILS approach subject (on course on path);

LOC ZONE 4 And ZONE 5 Roll Out Subject

The most challenging aspect of RFIS system is the LOC roll out flight testing, which requires higher precision for ILS/VOR receiver and synchronization performance for GNSS receiver. As shown in figure 12, the test curves of four roll out subjects indicate that RFIS system has good consistency and the curves fluctuation is within 2uA.

Note: Two different size antennas were used in the test, which caused a slight DDM deviation (within 1uA). As the drone approaches the LOC antenna, the displacement sensitivity decreases, and the positioning accuracy requirement for GNSS reference receiver becomes increasingly stringent.

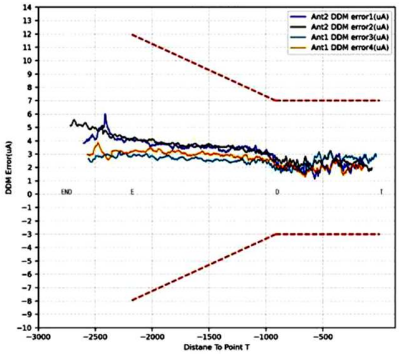

Figure 12. LOC ZONE 4 And ZONE 5 Roll Out Testing Curves

ILS Approach Subject

One more thing is about GS Zone 3 data processing. As shown in the figure, the processing of Zone 3 data is illustrated by Doc8071[3] and FAA8200[4]. The key issue is how to determine the structure tolerance limit of Zone 3. Both references show the use of an average calculation starting from point B/C to obtain an average path, but there is no clear definition of the average calculation process, such as what size of this average time window. Additionally, it is evident that if the data in Zone 3 is highly bended and jittered, the resulting average path line will also have significant follow-up bending and fluctuations.

If the structure tolerance limit is fluctuating, is it still a reasonable tolerance limit? In other words, what should the Zone 3 true path look like?

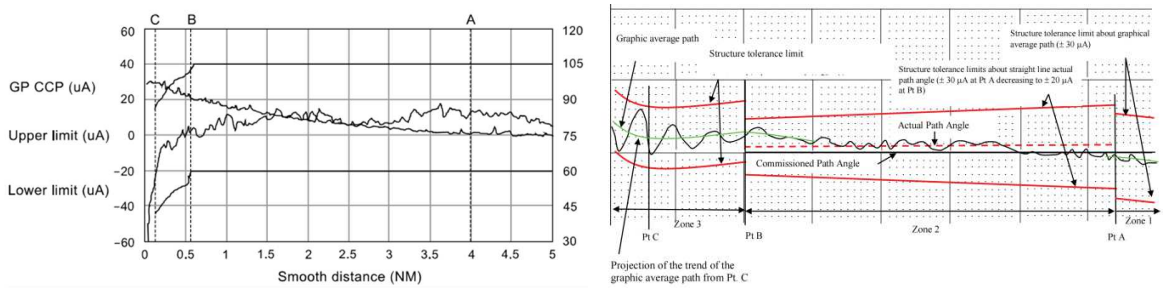

Figure 13. Glide Path Alignment Structure (from Doc8071 and FAA8200)

Many experts have conducted research and discussion on Zone3 data processing, and one of the more representative papers is the Ohio university paper《Assessment of the Effectiveness of the RDH/ARDH Evaluation Methodology for the ILS Glide Slope》.The article mainly discusses the calculation method for RDH/ARDH, which is also the method used by FAA. In the article multiple airports' Zone 3 processing results show that there is a significant pull-off in the Zone 3 path after updating the AP height. But the author did not provide a reasonable explanation.

GS Zone 3 Model Analysis

As is well known, practical GS path is a hyperbolic model, which represents the set of positions at which the DDM equals 0uA. This practical GS path has a significant positional deviation from the ideal downward straight line in Zone 3. It bends upwards. As shown in Figure 14 :

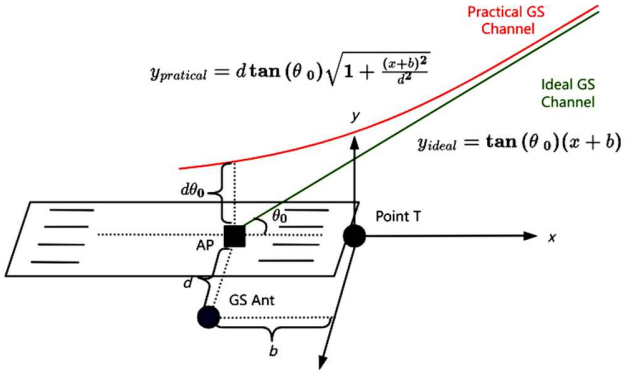

Figure 14. Glide Path Alignment Structure

Practical GS path: $y_{pratical} = d\tan(\theta_0)\sqrt{1+\frac{(x+b)^2}{d^2}}$ (1)

Ideal GS straight path: $y_{ideal} = \tan(\theta_0)(x+b)$ (2)

So the position deviation : $y_{pratical} - y_{ideal} = d\tan(\theta_0)\sqrt{1+\frac{(x+b)^2}{d^2}} - \tan(\theta_0)(x+b)$

Considering the displacement sensitivity and the width of the glide slope, the DDM error model should be:

$$DDM\_Error_{model} = \left[d\tan(\theta_0)\sqrt{1+\frac{(x+b)^2}{d^2}} - \tan(\theta_0)(x+b)\right] \times \frac{180}{(x+b)\pi} \times \frac{150}{GS_{width}} \quad (3)$$

in which:

d: distance between GS antenna and point AP;

θ_0: GS path angle (about 3 degree);

b: distance between point T and point AP.

GS_{width}: half width of GS (about 0.72 degree)

Since GS antenna position is fixed relative to runway, based on facility database , the initial values for those four parameters can be roughly determined. The height variable of point AP (△h) is unknown, which is also a topic often discussed by flight inspection experts.

So the height variable of point AP needs to be taken into account in formula (3), and the updated formula(4) is as follows:

$$DDM\_Error_{HOM} = \left[d\tan(\theta_0)\sqrt{1+\frac{(x+b)^2}{d^2}} - \tan(\theta_0)(x+b) - \Delta h\right] \times \frac{180}{(x+b)\pi} \times \frac{150}{GS_{width}} \quad (4)$$

Let's name the formula (4) as **Hyperbolic Optimization Model** and abbreviate **HOM**. The following discussion explores how to calculate the Zone 3 tolerance criterion using HOM model.

Data processing flow is as follows:

1. Through facility database, determine the initial values of parameters b, θ_0, d and GS_{width};

2. Substitute initial values into HOM model, and keep Δh as variable;

3. Use Zone 3 DDM error measurement results to perform fitting processing based on HOM model;

4. After fitting processing, obtain the value of Δh. This Δh is the correction amount for point AP height in the database;

5. Correct the height of point AP, re-calculate the DDM error measurement results, and repeat steps 1~3 to obtain the true Zone 3 Path line based on HOM model.

As mentioned process for calculating Zone 3 structure limit, an additional product Δh has been obtained, which is actually similar to the RDH calculation method, albeit based on Zone 2 data for RDH calculation and Zone 3 data for Δh calculation. The calculation process has been iterated once, and after the second calculation, the new Δh correction value will be close to zero.

Figure 15 shows the processing results for GS Zone 3 of 07L and 25R.

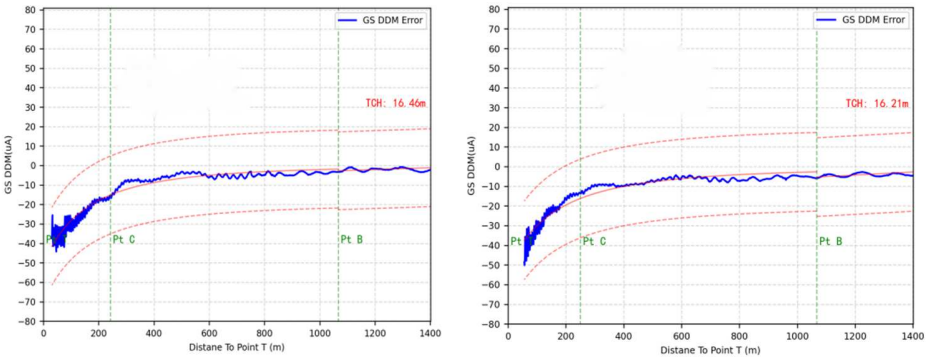

Figure 15. Processing Results for GS Zone 3 of 07L and 25R

CONCLUSIONS

After years of research and testing, the RFIS system has achieved the following results:

a. Ability to perform LOC and GS testing simultaneously;

b. The RFIS test results are consistent with the test results of flight inspection aircraft.

c. It is very meaningful for daily troubleshooting of ILS facility;

FUTURE WORK

The team will continue to carry out more facility testing, accumulate data, and further compare the results.

REFERENCES

[1] Moore T .Understanding GPS/GNSS: Principles and Applications, Third edition[J].The Aeronautical journal, 2019(Aug. TN.1266):123.

[2] DJI, PSDK Basic Introduction, 2023.

[3] FAA O, United Statues Standard Flight Inspection Manual [J]. FAA Order, 2005, 8200.

[4] Doc I, 8071 [J]. Volume I, Fifth Edition, 2018.

[5] Edwards J S , Dibenedetto M F .Assessment of the Effectiveness of the RDH/ARDH Evaluation Methodology for the ILS Glide Slope[J]. 2008.